Time-Resolved NMR Analysis of Proteolytic α-Synuclein Processing in vitro and in cellulo

Time-resolved NMR analysis of proteolytic α-synuclein processing *in vitro* and *in cellulo*

Antonio Limatola[1,3], Cedric Eichmann[1], Reeba Susan Jacob[1,4], Gili Ben-Nissan[2], Michal Sharon[2], Andres Binolfi[1,5] and Philipp Selenko[1,4]

[1] Leibniz Institute of Molecular Pharmacology (FMP-Berlin), In-cell NMR Group, Robert-Rössle Strasse 10, 13125 Berlin, Germany

[2] Department of Biomolecular Sciences, Weizmann Institute of Science, 234 Herzl Street, 761000 Rehovot, Israel

[3] present address: Department of Biology, Stanford University, Stanford, California 94305-5430, USA

[4] present address: Department of Biological Regulation, Weizmann Institute of Science, 234 Herzl Street, 761000 Rehovot, Israel

[5] present address: Instituto de Biología Molecular y Celular de Rosario (IBR-CONICET) and Plataforma Argentina de Biología Estructural y Metabolómica (PLABEM). Ocampo y Esmeralda, 2000, Rosario, Argentina.

to whom the correspondence should be addressed:

Received: 07 17, 2018; Revised: 09 14, 2018; Accepted: 09 25, 2018

This article has been accepted for publication and undergone full peer review but has not been through the copyediting, typesetting, pagination and proofreading process, which may lead to differences between this version and the Version of Record. Please cite this article as doi: 10.1002/pmic.201800056 .

binolfi@ibr-conicet.gov.ar and selenko@fmp-berlin.de

Abstract

Targeted proteolysis of the disordered Parkinson's disease protein alpha-synuclein (αSyn) constitutes an important event under physiological and pathological cell conditions. Here, we introduce the use of time-resolved nuclear magnetic resonance (NMR) spectroscopy to study site-specific αSyn cleavage by different endopeptidases *in vitro* and by endogenous proteases in extracts of challenged and unchallenged cells. Specifically, we analyze proteolytic processing under neutral and low pH conditions and in response to Rotenone-induced oxidative stress. We further interrogate time-dependent degradation of electroporation-delivered αSyn in intact SH-SY5Y and A2780 cells and, thereby, derive a general framework for NMR-based proteolysis studies *in vitro* and *in cellulo*. Our results confirm earlier reports pertaining to the exceptional proteolytic stability of αSyn under physiological cell conditions. However, we also observe enhanced protease susceptibilities in selected mammalian cell lines and upon induced cell stress.

Significance

Proteolytic processing of the disordered human amyloid and Parkinson's disease protein αSyn constitutes an important cellular event that determines multiple aspects of its aggregation behavior. At the same time, unbiased readouts of cellular protease activities acting on single protein substrates are difficult to obtain *in situ* because most methods require post-reaction processing to analyze individual sample fragments. We use NMR spectroscopy and isotope-labeled αSyn to directly follow its degradation in different *in vitro* and *in cellulo* environments. By being able to simultaneously monitor all αSyn residues in their native and cleaved forms, we detect proteolytic fragments side-by-side with intact αSyn molecules. Relative NMR signal intensities and changes thereof enable us to quantify individual protein species and allow us to follow protease cleavage reactions in a time-resolved manner with single amino-acid resolution.

1 Introduction

Protein turnover by targeted proteolysis regulates the lifetimes of proteomes in all kingdoms of life. Proteolytic processing of folded proteins typically requires local unfolding to provide access to protease substrate sites. Intrinsically disordered proteins (IDPs) lack stable secondary, tertiary and quaternary structures, and their intracellular proteolytic stabilities were thought to be greatly reduced. Proteome-wide lifetime studies in different species indicated that this is not strictly the case.[1] In turn, different routes to interrogate the proteolytic fate of individual IDPs are currently being explored. Analytical tools to study the stability of single proteins in cellular environments often suffer from incomplete coverage of produced truncation fragments, which relates to shortcomings in targeted detection methods such as in mass spectrometry-based approaches for example, or the lack of comprehensive antibody libraries to cover all possible combinations of epitope fragments by immunodetection.[2] Here, we assess the suitability of time-resolved NMR spectroscopy to directly monitor proteolytic processing of a canonical IDP substrate in different *in vitro* and cellular environments. Specifically, we follow cleavage of ^{15}N isotope-labeled alpha-synuclein (αSyn) in reconstituted protease reactions and by endogenous enzymes in cell-free extracts and intact cells.

Protease processing of the human Parkinson's disease (PD) protein αSyn plays important roles in its activity, homeostasis and cellular clearance.[3] In addition, proteolytic fragments of αSyn have been implicated in aggregate seeding and spreading, as well as primary or secondary causes of cytotoxicity.[4, 5, 6] Especially C-terminal truncations shown to occur under physiological and pathological cell conditions raised vested interest as PD-relevant agents, given that they aggregate readily *in vitro* and *in vivo* and act as potent enhancers of full-length αSyn oligomerization.[7, 8, 9] In turn, multiple proteases were shown to act on αSyn intra- and extracellularly, including matrix metalloproteases (MPPs), plasmin and neurosin.[10] Investigations into intracellular proteases targeting C-terminal αSyn sites such as calpains, cathepsins, caspases and asparagine endopeptidases remained at the center of attention, with several enticing disease connections emerging.[11] How these

proteolytic events contribute to PD onset, progression and/or pathology remains to be determined conclusively.

In 2016, we reported on the in-cell NMR behavior of electroporation-delivered αSyn in different neuronal and non-neuronal cell lines.[12, 13] In these studies, we observed little signs of intracellular αSyn degradation, typically after 5 hours of in-cell sample recovery and for up to 12 h of measurements in the NMR spectrometer, which agreed with biochemical studies reporting on the exceptional long half-life of αSyn in different mammalian cell types (~50 h).[14] In the present work, we sought to challenge this notion in two ways: First, we set out to assess the robustness of NMR spectroscopy to detect and report on proteolytic processing of αSyn, and, second, we aimed at establishing cellular conditions that deviated from the original behavior and led to intracellular αSyn degradation. In the first part of our results' section, we describe the NMR characteristics of site-selective αSyn cleavage in reconstituted protease reactions. In the second part of our study, we delineate the spectral features of proteolytic αSyn processing by endogenous enzymes in extracts of cells cultured under physiological and cellular oxidative stress conditions. Finally, we deduce the in-cell NMR signatures of αSyn proteolysis in neuronal SH-SY5Y and non-neuronal A2780 cells. Overall, we conclude that intracellular αSyn is indeed remarkably protease-resistant, especially in the absence of cytotoxic insults. We discuss these findings in relation to possible scenarios of cellular and organismal ageing, and how they might contribute to neurodegenerative disease states.

2 Materials and Methods

2.1 Expression and purification of recombinant αSyn

^{15}N isotope-labeled, N-terminally acetylated, human αSyn was prepared as described.[13] Methionine-oxidized ^{15}N isotope-labeled αSyn was generated from these samples as reported.[12] In brief, 2 mL of 500 μM recombinant protein was incubated with 4 % H_2O_2 (Sigma) for 2 h, followed by purification via size-exclusion chromatography. Complete peroxide removal was confirmed with a colorimetric

assay (Enzo Life Sciences). Quantitative αSyn oxidation was verified by 2D NMR spectroscopy. Protein concentrations were determined spectrophotometrically by absorbance measurements at 274 nm with ε = 5600 $M^{-1}cm^{-1}$. Final stock solutions of reduced and oxidized, ^{15}N isotope-labeled αSyn were prepared in 20 mM phosphate buffer, 150 mM NaCl at pH 7.0 (i.e. NMR Buffer). N-terminally acetylated αSyn was used throughout this study.

2.2 Proteases and reconstituted reactions

α-Chymotrypsin and Trypsin were purchased from UPS and Sigma, respectively. Reactions were carried out with 0.2 enzymatic units (U) of proteases in NMR buffer (10 % D_2O) at 25 °C. Proteinase K was obtained from NEB and used at 0.01 U in NMR buffer at 25 °C. Cathepsin D was purchased from Abcam and reactions were carried out at 0.15 µM of protease in 20 mM NaOAc, 50 mM NaCl, 5 mM DTT, 5 mM EDTA at pH 5.0 and 25 °C. Final NMR reaction volumes were 150 µL with 50 µM ^{15}N isotope-labeled αSyn as substrate. Cathepsin D and 20S Proteasome reactions were set up in 200 µL volumes, of which 10 µL were removed at different time points for sodium dodecyl sulfate (SDS) polyacrylamide gel (PAGE) analysis (see below).

2.3 NMR spectroscopy

All 2D ^{1}H-^{15}N correlation experiments were recorded with SOFAST-HMQC pulse-sequences on Bruker Avance spectrometers operating at 600 or 750 MHz and equipped with cryogenically cooled, triple resonance $^{1}H(^{13}C/^{15}N)$ TCI probes.[15] For reactions with commercial enzymes and purified 20S Proteasomes (**Figures 1** and **2**, **Suppl. Figures 1, 2** and **3**), 2D NMR spectra were recorded with 1024 (^{1}H) and 256 (^{15}N) complex points, 16 scans, 60 ms recycling delay, at the indicated temperatures and pH (acquisition time 20 min). For NMR experiments in pH 5.0 and pH 7.0 extracts of challenged and unchallenged SH-SY5Y cells (**Figure 3**), acquisition parameters were 1024 (^{1}H) and 256 (^{15}N) complex points and 64 scans, 30 ms recycling delay (acquisition time 40 min). Experiments in pH 7.0 extracts of unchallenged A2780, HeLa, SK-N-SH and SH-SY5Y cells (**Suppl. Figure 4**) were recorded with 2048 (^{1}H) and 512 (^{15}N) complex points and 16 scans, 60 ms recycling delay

(acquisition time 40 min). 2D in-cell NMR experiments in A2780 and SH-SY5Y cells (**Figure 4** and **Suppl. Figure 5**) were recorded with 1024 (^{1}H) and 128 (^{15}N) complex points, 2048 scans and 30 ms recycling delay at 10 °C. Nitrogen carrier frequencies and ^{15}N sweep-widths were adjusted to accommodate NMR degradation signals without aliasing. *In vitro* spectra were zero-filled to 4-times the number of real points and processed with sine-modulated window functions. In-cell NMR spectra were zero-filled to twice the number of real points and processed without applying a window function. Baseline corrections for proton and nitrogen dimensions were used for all spectra. Consecutive 2D NMR experiments were acquired for time-course analyses. For reconstituted protease reactions, kinetic profiles were determined by measuring cross-peak intensities of residues flanking the respective protease cleavage sites. Exponential decay or buildup functions were calculated in GraphPad Prism 5.0 analogous to described routines for delineating site-specific protein phosphorylation rates.[16] Unambiguous identification of individual protease substrate sites was based on identical signal intensity changes of cleaved and neighboring αSyn residues. Acquisition, processing and visualization of NMR spectra were carried out in TOPSPIN 3.2 (Bruker), SPARKY and iNMR.

2.4 αSyn peptides and peptide-protease reactions

N-terminal αSyn peptides 1- MDVFMK-6 (peptide 1) and 1- MDVFMKGLSKAKEGV-15 (peptide 2) were prepared by solid-phase peptide synthesis (SPPS) on Rink amide resin using Fmoc chemistry, purified by reverse-phase high-performance liquid chromatography (HPLC) on a Waters Delta 600, confirmed by electrospray ionization time-of-flight mass spectrometry (ESI-TOF-MS, Agilent) and NMR. Peptides were produced with amidated C- and acetylated N-termini. Peptide stocks (1 mM) were prepared by dissolving 0.4 and 0.84 mg of peptides 1 and 2, respectively, in 500 µL of pH-5 buffer. Complete ^{1}H chemical shift assignments were obtained by ^{1}H-^{1}H TOCSY experiments on solutions containing 100 µM of peptides and based on previous work.[17] Spectra were recorded on a 600 MHz Bruker Avance spectrometer equipped with a cryogenically cooled, triple resonance ^{1}H(^{13}C/^{15}N) TCI probe. Acquisition parameters were 1024 (^{1}H) and 256 (^{1}H) complex points, 70 ms

mixing time and 9.6 KHz spin-lock (sweep-width 10 p.p.m.). For Cathepsin D cleavage assays, 500 μL of 100 μM peptide solutions in pH-5 buffer were reacted with 0.15 μM of protease for 12 h. Upon completion, ^{1}H-^{1}H TOCSY experiments were repeated as described above.

2.5 Purification of 20S proteasomes

Rat liver 20S proteasomes were purified as described.[18] In brief, rat livers were homogenized in lysis buffer containing 20 mM Tris-HCL (pH 7.5), 1 mM EDTA, 1 mM dithiothreitol (DTT) and 250 mM sucrose. The lysate was centrifuged at 1,000 x g for 15 min at 4 °C. The supernatant was diluted to 400 mL with lysis buffer and the concentration of NaCl was adjusted to 0.5 M. The lysate was then ultra-centrifuged for 2.2 h at 152,000 x g and the resulting supernatant was centrifuged again at 200,000 x g for 6 h. The pellet containing the proteasomes was resuspended in 20 mM Tris-HCl (pH 7.5) and loaded onto 1.8 L Sepharose 4B resin. Eluted fractions containing the 20S proteasome were identified by their ability to hydrolyze the fluorogenic peptide suc-LLVY-AMC, in the presence of 0.02 % SDS. 20S proteasome-containing fractions were combined and loaded onto three successive anion exchange columns: Source 15Q, HiTrap DEAE FF and Mono Q 5/50 GL (GE Healthcare). Elution was performed with a 0-1 M NaCl gradient. Positive fractions were combined and buffer exchanged to 10 mM phosphate buffer (pH 7.4) containing 10 mM $MgCl_2$, using a 10 kDa concentrator (GE Healthcare). Samples were then loaded onto a ceramic hydroxyapatite column (Bio-Rad) and 20S proteasomes were eluted using a linear gradient of 10-400 mM phosphate buffer. Purified 20S proteasomes were analyzed by SDS–PAGE and activity assays. Stock concentrations were adjusted to 2 μM of total protein. αSyn reactions were carried out with 50 μM of ^{15}N isotope-labeled protein and 0.1 μM of 20S proteasomes in 20 mM phosphate buffer, 150 mM NaCl, 5 mM DTT at pH 7.0 and 25 °C.

2.6 SDS-PAGE and Western blotting

For Cathepsin D and 20S proteasome experiments, 10 μL reaction aliquots were removed at the indicated time-points and boiled in Laemmli buffer for 10 min. Samples were loaded onto 4-20 %

precast gradient gels (Bio-Rad), separated and stained with Coomassie Brilliant Blue (Sigma). For Western blotting of αSyn samples in extracts of Rotenone-challenged SH-SY5Y cells, 128 ng of ^{15}N isotope-labeled protein was incubated with soluble extract fractions (4.3 mg/mL total protein) for the indicated time periods. For Western blotting of SH-SY5Y in-cell NMR sample lysates, 2 x 10^5 electroporated cells were subjected to five freeze-thaw cycles on dry-ice/ethanol. Soluble and insoluble fractions from were separated by centrifugation at 16,000 x g for 10 min at 4 °C. All extract and lysate samples were boiled in Laemmli buffer, separated on 4-20 % precast gradient gels (Bio-Rad) and transferred onto polyvinylidene difluoride (PVDF) membranes by semi-dry blotting (Trans-Blot Turbo, BioRad). For in-cell NMR lysates, a dilution series of 64-256 ng of recombinant αSyn was loaded as input control. Membranes were fixed with 4 % paraformaldehyde for 15 min, washed with PBS and blocked in 5 % non-fat dry milk in TBS-T for 1 h at room temperature. Blots were incubated with one of the following primary antibodies as indicated (overnight at 4 °C). Rabbit monoclonal anti-αSyn ab51252 (Abcam), unspecified N-terminal epitope, used at 1:1000 dilution. Mouse monoclonal anti-αSyn sc69977 (Santa Cruz), unspecified C-terminal epitope, used at 1:200 dilution. Mouse monoclonal anti-αSyn sc12767 (Santa Cruz) C-terminal epitope comprising residues 121-125, used at 1:200 dilution. After washing with PBS and TBS-T (2 x 5 min each), appropriate horseradish peroxidase (hrp)-conjugated secondary antibodies were applied for 1 h at room temperature (1:10000 dilutions). Membranes were washed with TBS-T (3 x 5 min each) and probed with SuperSignal West chemiluminescent substrate (Thermo Scientific). Luminescence was detected on a Bio-Rad Molecular Imager with the ImageLab software (Bio-Rad).

2.7 Cell lines, Rotenone treatment and cell extracts

A2780, HeLa and SK-N-SH cells were obtained and cultured as previously described.[13] SH-SY5Y cells we purchased from ATCC and maintained in DMEM-Ham's F-12 (Biochrom) growth media, supplemented with 10 % fetal bovine serum (FBS, Biochrom). Rotenone was purchased from Sigma, dissolved in 100 % DMSO and added to cultured SH-SY5Y cells at final concentrations of 100 nM for 72 h, following published protocols to induce cellular oxidative stress.[19, 20] For extract

preparation, cells were grown to ~80 % confluence in 165-cm^2 culture dishes at 37 °C, 5 % CO_2, scrapped off with a rubber policeman and collected in 50 mL Falcon tubes by centrifugation at 1.000 x g for 5 min. Pellets were resuspended in 2 volumes of hypotonic detergent buffer containing 45 mM HEPES (for pH 7.2 extracts), or 45 mM NaOAc (for pH 5.0 extracts) and 0.5 mM EDTA, 10 mM $MgCl_2$, 50 mM KCl, 3 % (vol/vol) NP-40, 3 mM DTT. Soluble extract fractions were obtained by centrifugation at 16.000 x g at 4 °C for 10 min. Total protein concentrations were determined with a Bradford assay (Bio-Rad). Cell extracts were used immediately or aliquoted, snap-frozen in liquid nitrogen and stored at -80 °C. For NMR experiments in cell extracts, ^{15}N isotope-labeled αSyn was directly added to final concentrations of 50 μM.

2.8 In-cell NMR samples

In-cell NMR samples were prepared according to the protocol by Theillet *et al.*.[13] In brief, we electroporated 400 μM ^{15}N isotope-labeled αSyn into 100 x 10^6 A2780 and SH-SY5Y cells, grown in RPMI 1640 (Millipore) and DMEM-Ham's F-12 (Biochrom) growth media, respectively, supplemented with 10 % fetal bovine serum (FBS, Biochrom). 100 μL aliquots of the electroporation mixtures were pulsed twice with an Amaxa nucleofector (Lonza). Electroporated cells were washed by low-speed centrifugation and sedimentation to separate non-transduced αSyn. Cells were returned to the CO_2 incubator for recovery periods of 5 or 12 h at 37 °C. For NMR measurements, cells were washed with pre-warmed PBS, detached with trypsin and subsequently washed once with pre-warmed pH-stable Leibowitz's L-15medium (Gibco) supplemented with 10% FBS and resuspended in Leibowitz's L-15 medium, containing 10 % FBS and 10 % D_2O. ~80 x 10^6 cells were transferred to 4 mm Shigemi NMR tubes for in-cell NMR experiments without applying the plunger (see above).

2.9 Bright-field and immunofluorescence (IF) microscopy

Morphologies of cultured cells were routinely checked by bright field microscopy on a Nikon Eclipse TS100 at 10x magnification. Images of Rotenone-challenged SH-SY5Y cells were acquired at regular intervals during 72 h of toxin exposure to confirm overall cell viability. Electroporated cells used for

IF microscopy were prepared analogous to in-cell NMR samples with 400 μM of ^{15}N isotope-labeled αSyn. After electroporation, ~1 x 10^5 SH-SY5Y or ~5 x 10^5 A2780 cells were seeded onto collagen (10 μg/cm^2), or fibronectin (1 μg/cm^2) coated 25 mm cover slips, respectively, and allowed to recover for 5 h at 37 °C in the CO_2 incubator. 5 h-recovery cells were washed 3-times with PBS and fixed in PBS containing 4 % (w/v) PFA for 15 min. 12 h-recovery cells were washed twice with PBS, replenished with fresh media and returned to the incubator for an additional 7 h. Following 12 h of incubation, these cells were fixed as described above. Cells were permeabilized with 0.1 % (v/v) Triton-X in PBS for 3 min, washed 3-times with PBS and blocked with 0.13 % (v/v) of cold fish skin gelatin (Sigma) in PBS for 1 h. Subsequently, cells were incubated with ab51252 anti-αSyn primary antibody (Abcam, 1:200 dilution in blocking buffer) at room temperature for 2 h. Following, coverslips were washed 3-times with PBS and cells were incubated with Atto647-coupled, anti-rabbit secondary antibody (Sigma, 1:1000 dilution) and fluorescein isothiocyanate (FITC)-labeled phalloidin (Millipore, 2 μg/mL) at room temperature for 1 h. Cover slips were washed with PBS and cell nuclei were counterstained with 1 μg/mL 4',6-diamidino-2-phenylindole (DAPI, Invitrogen) in PBS for 5 min. After washing once in PBS, cover slips were mounted with ImmuMount (Thermo Scientific). Confocal images were taken at 20-, 40- and 60-fold magnification with excitation wavelengths of 405, 488, and 633 nm on a Zeiss LSM 510 META laser-scanning microscope.

3 Results

Residue-resolved protein NMR signals are sensitive indicators of their immediate chemical environments. NMR resonances and their chemical shifts (δ) report on the conformational and functional states of individual amino acids, whereas chemical shift changes (Δδ) are routinely used to interrogate changes in secondary and tertiary structure, or to identify site-specific post-translational modifications (PTMs) such as phosphorylation, acylation, alkylation, glycosylation or oxidation.[12, 21] These modifications alter the chemical environments of individual residues in highly characteristic manners, with resulting Δδ's providing qualitative and quantitative information about progressive changes in protein structure, function and corresponding PTM states. In combination with fast pulse

sequences and advanced sampling schemes, two-dimensional (2D) NMR spectra containing such residue-resolved chemical shifts can be obtained within seconds to minutes.[15, 22] Consecutive 2D NMR experiments then enable 'real-time' monitoring of biological processes ranging from enzyme reactions to protein folding.[23, 24]

In a first step, we set out to determine whether we can employ the same rationale to characterize protease-mediated protein cleavage by NMR spectroscopy. Most proteases (i.e. endopeptidases) catalyze the hydrolysis of individual backbone amide bonds, which produces peptide fragments with new alpha-amino (NH_3^+) and carboxy-terminal (COO^-) ends (**Figure 1A**). Such fragmentation drastically alters the chemical environments of surrounding residues, which we speculated should lead to equally large and readily identifiable chemical shift changes. In uniformly ^{15}N isotope-labeled proteins, newly created N-termini may not be detected in 2D ^{1}H-^{15}N correlation experiments due to fast exchange with solvent protons at neutral pH (**Figure 1B**). By contrast, backbone amide resonances of proteolytically produced C-termini are expected in regions of 2D ^{1}H-^{15}N spectra that are shifted upfield in the proton (^{1}H) and downfield in the nitrogen (^{15}N) dimensions due to shielding and de-shielding of ^{1}H and ^{15}N tensors, respectively. *In situ* NMR measurements of such reactions by using ^{15}N isotope-labeled protein substrates and unlabeled proteases may thus be analyzed in a time-resolved fashion to map individual substrate sites and deduce their rates of proteolysis (**Figure 1C**).

3.1 αSyn cleavage by Chymotrypsin, Trypsin and Proteinase K

For an initial proof-of-principle, we added defined amounts of commercial proteases to ^{15}N isotope-labeled, N-terminally acetylated αSyn and followed proteolytic processing via time-series of consecutive 2D ^{1}H-^{15}N experiments. First, we reacted αSyn with α-Chymotrypsin, a generic protease that preferentially cleaves peptide amide bonds C-terminal to aromatic residues, i.e., tyrosines, phenylalanines and tryptophanes. αSyn contains four tyrosine (Y39, Y125, Y133, Y136), two phenylalanine (F4, F94) and no tryptophane residues (**Suppl. Figure 1A**). In line with the expected NMR characteristics, we observed proteolytic processing of αSyn in time-resolved NMR

experiments, manifested by the progressive appearance of new NMR signals in the aforementioned 'degradation' region of corresponding 2D NMR spectra (**Figure 1D-F**). By using combined chemical shift difference mapping of disappearing N- and new C-terminal NMR signals, we identified Y39, F4, F94, Y125 and Y133 as the respective Chymotrypsin cleavage sites on αSyn. Cleavage at Y39 occurred the fastest and was observed first (**Figure 1D**). Specifically, we detected line-broadening of new N-terminal signals V40, G41, S42 and K43, whereas T44 was shifted to a new position. By contrast, the NMR peak of C-terminal Y39 was clearly off-set, while resonances of L38, V37 and G36 displayed notable chemical shift changes. With time, NMR spectra revealed cleavage at F4 and F94, manifested by the appearance of similarly off-set resonances in the degradation region (**Figure 1E**). These changes were paralleled by line broadening of new N-terminal signals M1, D2 and V3, reporting on F4 cleavage, and of V95, K96 reporting on F94 processing. Corresponding chemical shift changes of C-terminal residues K6, G7, L8, S9 (for F4) and G93, T92, A91-89 (for F94) completed the picture. Finally, simultaneous cleavage at Y125 and Y133 led to line-broadening of E126, M127 (N-terminal) and chemical shift changes of Y125, A124, E123 and N122, as well as Y133, E130 and S129 (C-terminal), respectively (**Figure 1F**). These results recapitulated the NMR behavior predicted by theory. Surprisingly, however, our data also implied that the different aromatic residues of αSyn did not constitute equivalent substrate sites and that Chymotrypsin processing followed the order Y39 >> F4 > F94 > Y125, Y133. To substantiate our conclusion, we measured combined NMR signal intensity changes and fitted them to first-order rate kinetics to delineate time- and residue-resolved cleavage profiles along previously published protocols (**Figure 1G**).[16] Indeed, our analysis confirmed that Chymotrypsin discriminated between individual αSyn substrate sites and processed them with different apparent rates.

To further assess the analytical power of NMR as a tool for studying protease reactions, we set up similar experiments with ^{15}N isotope-labeled αSyn and unlabeled Trypsin. Trypsin cleaves peptide bonds C-terminal of lysine and arginine residues, of which αSyn contains 15 and none, respectively. αSyn lysines feature prominently in the six imperfect KTK-E/Q-GV repeats that span residues 1-80 of the protein where they contribute to membrane binding (**Suppl. Figure 1B**).[25] Given

the large number of protease substrate sites, Trypsin cleavage produced multiple αSyn fragments (**Suppl. Figure 1C**). Instead of determining the identities of individual fragments, we focused on vanishing NMR signals to annotate primary Trypsin sites. Early reaction time-points revealed absent or shifted αSyn resonances for residues M1-K12, suggesting that initial processing occurred at N-terminal K6, K10 and probably K12. At later time-points, signals encompassing K21, K23, K43, K45 and K80 displayed chemical shift changes or line broadening. Interestingly, lysine resonances of K58, K60, K96, K97 and K102 remained unchanged even after extended enzyme incubation, which indicated that no cleavage occurred at these sites. In summary, our results established that individual KTK-E/Q-GV repeats did not constitute equivalent Trypsin substrate sites and that processing pursued in a non-random fashion. Finally, we reacted ^{15}N isotope-labeled αSyn with catalytic amounts of Proteinase K (**Suppl. Figure 2**), a broadly acting enzyme that cleaves peptide bonds C-terminal to aliphatic and aromatic residues, but without clear sequence specificity. Time-resolved NMR spectra revealed extensive αSyn cleavage at multiple sites. Different to Chymotrypsin and Trypsin reactions though, newly generated αSyn fragments displayed transient resonance signals that progressively changed in the course of the reaction. This suggested that initial fragments were further processed by Proteinase K. On a qualitative level, Trypsin and Proteinase K results supported our previous conclusions regarding the robustness with which protease cleavage reactions can be monitored by time-resolved NMR spectroscopy.

3.2 αSyn cleavage by Cathepsin D and the 20S proteasome

Next, we turned to proteases that are directly relevant to αSyn's biology. Specifically, we set up reactions with recombinant Cathepsin D and purified 20S proteasomes. Both systems have been implicated in the cellular clearance of αSyn, either via lysosomal chaperone-mediated autophagy or the cytoplasmic ubiquitin-proteasome machinery, respectively.[4] In agreement with the low pH requirements for Cathepsin D as a lysosomal enzyme, we did not observe αSyn cleavage at pH 6.4 and above, whereas the protease efficiently processed αSyn at pH 5 (**Figure 2A**). We therefore performed all Cathepsin-NMR experiments at this pH. Accordingly, line broadening of newly

generated αSyn N-termini was less severe than at neutral pH. NMR spectra of the Cathepsin D cleavage reaction revealed site-selective processing of F4 and F94 (**Figure 2B** and **Suppl. Figure 3A**), which resulted in NMR characteristics reminiscent of the same-site processing by Chymotrypsin (see **Figure 1E** for comparison). Cleavage of both residues occurred at similar rates, although proteolysis at F4 was detected before F94 (**Suppl. Figure 3A**). To confirm chemical shift changes of residues N-terminal to F4, we ran similar Cathepsin D experiments on unlabeled αSyn peptides spanning residues 1-6 and 1-15 and analyzed resulting fragments by ^{1}H-^{1}H 2D TOCSY experiments (**Suppl. Figure 3B**). Next, we asked whether post-translational modifications in the vicinity of F4 and F94 affected αSyn processing by Cathepsin D. Specifically, we sought to evaluate the effect of N-terminal methionine M1 and M5 oxidation on F4 cleavage. Methionine-oxidized αSyn is abundantly found in Lewy body aggregates of Parkinson's disease patients and serves as a proxy for reactive oxygen species accumulation in response to sustained cellular oxidative stress. We reacted methionine-oxidized αSyn with Cathepsin D and found that F4 cleavage was effectively abolished, whereas proteolysis at F94 was unchanged (**Suppl. Figure 3C**). This suggested that lysosomal processing of oxidation-damaged αSyn by Cathepsin D and other proteases may be altered.[26] Finally, we studied ubiquitin-independent αSyn degradation by 20S proteasomes that we purified from rat liver. In line with previous results, we detected exhaustive cleavage of αSyn at multiple sites, which yielded several protein fragments (**Figure 2C**). Instead of characterizing individual fragment identities, we focused on NMR resonances that remained unchanged, aiming to annotate regions of αSyn that were stably preserved upon 20S proteasome processing (**Figure 2D**). This analysis revealed that NMR signals of N-terminal αSyn residues M1, D2 and V3 retained their original peak positions, whereas F4-A17 vanished, or displayed major chemical shift changes. Similarly, amino acids spanning the N-terminus of the central aggregation-prone non-amyloid component (NAC) region, residues 60-88, were largely unaffected, whereas NMR signals of A89-F94 were absent. Several C-terminal αSyn residues, including A107, Q109, L113, D115, D121, N122, E137 and A140 remained unchanged, indicating that 20S degradation likely pursued from the N- to the C-terminus of the protein, along the known mechanism of αSyn-proteasome processing.[26] Our results also indicated

that proteasomes did not exhaustively degrade αSyn but yielded stable fragments with possible functions as dominant negative regulators. A similar behavior was recently reported for 20S processing of the mostly disordered, human transcription factor and oncoprotein p53.[27] Overall, the observed NMR degradation pattern was unique and did not resemble any of the previous protease reactions. This provided compelling evidence for the ability to distinguish between the proteolytic activities of different enzymes by NMR spectroscopy.

3.3 αSyn cleavage by endogenous protease in mammalian cell extracts and intact cells

To investigate the proteolytic stability of αSyn in cellular environments, we prepared extracts from cultured mammalian cells grown under physiological conditions i.e., in a non-stressed manner. Importantly, we did not add protease inhibitors to these extracts in order to interrogate full-scale effects of endogenous cellular enzymes. Contrary to our expectations regarding the proteolytic stability of a disordered protein in such environments, we found that αSyn was surprisingly protease resistant. Indeed, we detected no signs of protein degradation in HeLa, SH-SY5Y and SK-N-HS extracts, even after extended incubation and despite total protein concentrations in the range of 15-30 mg/mL (**Suppl. Figure 4**). To confirm that these extracts were biologically active and displayed general protease activities, we shifted the pH to 5 before adding αSyn. As shown for SH-SY5Y extracts, we noted rapid protein degradation, which stably persisted at dilute extract concentrations (1 mg/mL) (**Figure 3A**). NMR signals of C-terminal αSyn residues Q134-A140 were absent and we detected multiple degradation peaks at new resonance positions. A2780, HeLa and SK-N-SH extracts exhibited similar behaviors at low pH. These results established that aSyn did not constitute a preferred target for endogenous proteases in pH-neutral extracts of cells grown under physiological conditions. To test whether degradation properties changed in the presence of cellular oxidative stress, we incubated SH-SY5Y cells with the mitochondrial electron-transport chain inhibitor Rotenone (100 nM for 72 h) before preparing extracts.[20] Under these conditions, cells displayed clear signs of cytotoxity including bloated cell bodies and raffled plasma membranes (**Figure 3B**). At low pH and dilute extract concentrations (1 mg/mL), NMR spectra revealed massive αSyn degradation and a

multitude of new resonance signals including the ones that we observed in the absence of Rotenone treatment (compare **Figure 3C** and **Figure 3A**). At neutral pH, extracts of Rotenone-treated SH-SY5Y cells exhibited reduced αSyn degradation and few of the NMR features matched the low pH characteristics (**Figure 3D**). Line broadening was particularly evident for N-terminal αSyn residues M1-K12, the region spanning K80 to S87 and at amino acids D98-N103. Most prominently, the NMR signal of the last αSyn residue A140 displayed consistent peak splitting, similar to 20S proteasome reactions (**Figure 2D**) and hinting towards C-terminal truncation(s). We confirmed this hypothesis by Western blotting using antibodies against N- and C-terminal αSyn epitopes (**Figure 3E**).

Finally, we turned to intact SH-SY5Y cells to determine the proteolytic fate of electroporation-delivered, intracellular αSyn. We chose SH-SY5Y cells because our previous in-cell NMR experiments did not reveal indications for αSyn proteolysis in A2780, HeLa, RCSN-3, B65 and SK-N-SH cells within a time-frame of ~15 h after protein transduction by electroporation.[13] Similar to those results, in-cell NMR spectra of αSyn in SH-SY5Y cells showed minor signs of proteolysis after a recovery period of 5 h (**Figure 4A**) and we observed uniform line broadening of its first 10 residues caused by hydrophobic interactions with cytoplasmic components including proteins and membranes, as reported previously.[13] Allowing SH-SY5Y cells to recover for 12 h after electroporation produced a very different outcome and in-cell NMR spectra revealed greatly reduced signal intensities, suggesting that delivered αSyn had been efficiently cleared (**Figure 4B**). These findings were in stark contrast to results in A2780, HeLa, RCSN-3, B65 and SK-N-SH cells, in which we confirmed a protein half-life of ~50 h.[13] Remaining in-cell NMR resonances of αSyn displayed varying degrees of line broadening with signals corresponding to a continuous stretch of residues spanning D119 to S129 being greatly reduced (**Figure 4B**), hinting to possible cleavage events in this part of the protein. Conspicuously, C-terminal truncation of αSyn at D119, N122 and E123 has previously been identified to occur as a physiological cellular process.[8, 9] We confirmed αSyn clearance from SH-SY5Y by immunofluorescence (IF) microscopy and Western blotting, which also revealed that a substantial portion of the protein was present in the insoluble lysate fraction of cells

recovered for 5 h (**Figure 4C**). Moreover, most of the insoluble αSyn formed SDS-resistant, high-molecular weight aggregates, which we had not observed in other cells.[13] We did not detect αSyn aggregates in lysates of SH-SY5Y cells allowed to recover for 12 h, which suggested that these species had been efficiently cleared. By contrast, C-terminal truncation was evident for non-aggregated αSyn in the insoluble fraction. Adverse cellular toxicity precluded in-cell NMR investigations of this behavior in intact Rotenone-challenged SH-SY5Y cells.

Different to SH-SY5Y cells, in-cell NMR spectra of αSyn in A2780 cells after 12 h of recovery were of excellent quality and we only detected minor reductions in overall αSyn levels (**Suppl. Figure 5A**). Nonetheless, NMR spectra revealed site-selective line broadening of similar sets of C-terminal αSyn residues and peak splitting of penultimate A140 with a new resonance signal at a position similar to the one that we observed in SH-SY5Y cells (**Figure 4B**). Immunofluorescence microscopy did not provide evidence for αSyn aggregation, typically manifested by bright intracellular puncta (**Suppl. Figure 5B**). In addition, we did not detect SDS-resistant αSyn aggregates by Western blotting of A2780 cell lysates and little signs of C-terminal truncation (**Suppl. Figure 5C**). In summary, these findings established that the lifetimes of exogenously delivered αSyn varied between different mammalian cell lines and that intracellular stability, aggregation and clearance may be affected by cell type-specific factors.

4 Discussion

In this study, we sought to determine the analytical power of NMR spectroscopy to delineate qualitative and quantitative insights into the site-specific activities of different proteases *in vitro* and *in cellulo*. More specifically, we set out to evaluate this property on a protein substrate with little to no secondary or tertiary structure in its free forms, collectively referred to as an intrinsically disordered protein (IDP). To this end, we employed the classical IDP αSyn as a model substrate. Our results showed that NMR is well suited to monitor the activities of different proteases acting on αSyn with high confidence. For reconstituted protease reactions with single enzymes (**Figures 1, 2B**, **Suppl.**

Figures 1 and **3**), we found that cleavage at a few sites yielded well interpretable NMR spectra that allowed us to map individual substrate residues in an unambiguous manner. We accomplished this task by measuring NMR signal intensity changes in 2D ^{1}H-^{15}N NMR spectra, without the need for doubly ^{13}C and ^{15}N isotope-labeled NMR samples, lengthy 3D NMR experiments and re-assignment of backbone amide resonances. Importantly, we did so by following the same rationale that we had used to monitor other types of protein modifications such as phosphorylation, acetylation or methylation.[16, 21] Thereby, we extended previous conclusions regarding the versatility of the NMR chemical shift as a general tool to report on changes in the chemistries of individual protein residues.[23] Whenever protease cleavage reactions entailed multiple cleavage sites (**Figure 2B**, **Suppl. Figure 1** and **2**), qualitative and quantitative assessments of individual chemical shift changes and corresponding fragment identities became increasingly difficult to resolve. While we did no attempt to assign newly generated resonances with ^{13}C-^{15}N labeled samples and re-assignments of backbone resonances, we believe that such procedures are indeed feasible. We base this conclusion on two observations. First, endpoint states of protease reactions and their corresponding NMR spectra turned out to be surprisingly 'stable', which we think reflects the stringency of protease activities with few off-target effects once all substrate sites are processed. Second, newly formed αSyn fragments generally displayed greater chemical shift dispersions than the intact protein, which, together with the aforementioned properties of fragment stability, should make assignments via triple resonance experiments straightforward.

NMR experiments in intact SH-SY5Y and A2780 cells revealed fewer degradation features, suggesting that proteolytic αSyn processing under physiological cell conditions does not constitute a major metabolic event (**Figure 4** and **Suppl. Figure 5**). In SH-SY5Y cells, however, we detected broadly reduced NMR signal intensities after 12 h of recovery and minor signs of C-terminal truncation. In line with Western blotting results showing the presence of αSyn aggregates before cellular clearance (**Figure 4C**), this may indicate that αSyn cleavage leads to aggregation and, in turn, active removal of aggregated species. From an NMR point of view, such a scenario would explain the absence of detectable αSyn fragments in SH-SY5Y cells as their conversion into high molecular-

weight aggregates renders them NMR-invisible. Aggregate clearance may drive further aggregation and result in the progressive loss of NMR signals of monomeric αSyn (**Figure 4A, B**). Interestingly, this truncation-aggregation-clearance mechanism appeared to depend on the intactness of cells, as well as their identities. While we did not observe C-terminal processing of αSyn in pH-neutral SH-SY5Y cell extracts (**Suppl. Figure 4**), signal attenuation and aggregation were evident in intact SH-SY5Y but not in A2780 cells, despite similar NMR degradation signatures in both samples (**Figure 4** and **Suppl. Figure 5**). These findings provide additional evidence in support of cell type-specific contributions to αSyn's biological and pathological behavior in different intracellular milieus.[28] They further underscore the exquisite complementarity of extract and in-cell NMR measurements in delineating such comparative insights.

For Cathepsin D reactions, we showed that post-translational modifications in the vicinity of protease substrate sites, such as oxidation of αSyn methionines M1 and M5 for example, abolished proteolytic processing of neighboring residues, specifically cleavage at phenylalanine F4 (**Suppl. Figure 3C**). These results established that secondary modifications have the capacity to reprogram protease cleavage patterns and, thereby, redefine the identities of resulting substrate fragments. With respect to physiological clearance processes of αSyn, this may have grave consequences.[4] For instance, αSyn phosphorylation sites cluster around C-terminal residues Y125 to Y136, including serine S129, which is exclusively found in its phosphorylated form in Lewy body inclusions of Parkinson's disease patients.[6] At the same time, most cellular proteases also target C-terminal αSyn residues with D119 to N123 as the primary cleavage hotspots.[8] Whether and how phosphorylation affects proteolytic processing of these sites is not known. Similarly, the effects of methionine M116 and M127 oxidation on αSyn homeostasis have not been addressed.[12] Therefore, secondary changes in αSyn modifications, brought about by alterations during cellular and organismal ageing for example, may add to insults that affect the fidelity of primary cellular clearance systems and, thereby, contribute to disease development and the accumulation of toxic intracellular αSyn inclusions.

Regarding general IDP biology, our data confirmed that disordered αSyn constitutes an excellent substrate for different proteases *in vitro*. Reconstituted reactions revealed efficient proteolytic processing and rapid degradation into defined protein fragments (**Figures 1, 2** and **Suppl. Figures 1-3**). By contrast, αSyn proved remarkably stable in pH-neutral extracts of non-challenged mammalian cells (**Suppl. Figure 4**), despite an abundance of endogenous proteases as corroborated by extensive degradation under low pH conditions (**Figure 3**). This suggested that structural disorder *per se* does not impair the proteolytic stability of αSyn, underscoring the importance of IDP sequence contexts in determining general protease susceptibilities.[1] Proteolytic processing of αSyn in intact SH-SY5Y and A2780 cells revealed cell type-specific differences in overall activities (**Figure 4** and **Suppl. Figure 5**). While this may be attributed to a lower intracellular pH in SH-SY5Y than in A2780 cells (see pH arguments above), the known pH sensitivity of the αSyn histidine H50 chemical shift clearly established that the protein experienced similar low pH environments in both cell types. Therefore, the observed effects likely reflect genuine biological differences of these cellular milieus. In general terms, this raises important questions regarding the choice of relevant systems for studying basic biological processes. For αSyn, it highlights the need for comparative analyses in different cell types, for which the outlined NMR approach may prove highly valuable. What is the outlook for studying proteolytic processing of folded proteins along the same rationale? Clearly, secondary chemical shift changes due to the disruption of tertiary and/or quaternary structure may result in NMR behaviors that are more complex than what is seen by localized chemical alterations at individual residues in fully disordered proteins. However, it has been understood for some time that even folded proteins and protein domains display strong preferences for proteolytic processing at disordered substrate sites (i.e. providing optimal access for proteases), which typically reside in intradomain loop regions or within interdomain linker segments.[29] Following cleavage at these sites, stable protein fragments are usually generated, which has been exploited in limited proteolysis experiments for decades.[30] Therefore, we expect that NMR monitoring of proteolysis reactions of folded protein substrates will be equally feasible and offer similar benefits. Our own preliminary results in this direction indicate that this is indeed the case.

Supporting Information

Supporting Information is available at the Wiley Online Library or by the authors.

Acknowledgements

We thank Dr. Peter Schmieder and Monika Beerbaum for excellent maintenance of the NMR infrastructure and Dr. David Mulvihill for sharing the yeast NatB acetylase expression plasmid. A.B. thanks Claudio O. Fernández for helpful discussions. P.S. acknowledges funding by the ERC Consolidator Grant #647474 NeuroInCellNMR.

Conflict of Interests

The authors declare no conflict of interest.

5 References

[1] P. Tompa, J. Prilusky, I. Silman, J. L. Sussman, *Proteins* **2008**, *71*, 903; R. van der Lee, B. Lang, K. Kruse, J. Gsponer, N. Sanchez de Groot, M. A. Huynen, A. Matouschek, M. Fuxreiter, M. M. Babu, *Cell Rep.* **2014**, *8*, 1832.

[2] A. Tholey, A. Becker, *Biochim. Biophys. Acta* **2017**, *1864*, 2191.

[3] H. A. Lashuel, C. R. Overk, A. Oueslati, E. Masliah, *Nat. Rev. Neurosci.* **2013**, *14*, 38.

[4] A. M. Cuervo, E. S. Wong, M. Martinez-Vicente, *Mov. Disord.* **2010**, *25 Suppl 1*, S49.

[5] T. Lopes da Fonseca, A. Villar-Pique, T. F. Outeiro, *Biomolecules* **2015**, *5*, 435; A. Oueslati, M. Ximerakis, K. Vekrellis, *Exp. Neurobiol.* **2014**, *23*, 324.

[6] A. Oueslati, M. Fournier, H. A. Lashuel, *Prog. Brain Res.* **2010**, *183*, 115.

[7] M. Baba, S. Nakajo, P. H. Tu, T. Tomita, K. Nakaya, V. M. Lee, J. Q. Trojanowski, T. Iwatsubo, *Am. J. Pathol.* **1998**, *152*, 879; F. Bassil, P. O. Fernagut, E. Bezard, A. Pruvost, T. Leste-Lasserre, Q. Q. Hoang, D. Ringe, G. A. Petsko, W. G. Meissner, *Proc. Natl. Acad. Sci. U. S. A.* **2016**, *113*, 9593; W. Hoyer, D. Cherny, V. Subramaniam, T. M. Jovin, *Biochemistry* **2004**, *43*, 16233; G. K. Tofaris, P. Garcia Reitbock, T. Humby, S. L. Lambourne, M. O'Connell, B. Ghetti, H. Gossage, P. C. Emson, L. S. Wilkinson, M. Goedert, M. G. Spillantini, *J. Neurosci.* **2006**, *26*, 3942; A. Ulusoy, F. Febbraro, P. H. Jensen, D. Kirik, M. Romero-Ramos, *Eur. J. Neurosci.* **2010**, *32*, 409.

[8] W. Li, N. West, E. Colla, O. Pletnikova, J. C. Troncoso, L. Marsh, T. M. Dawson, P. Jakala, T. Hartmann, D. L. Price, M. K. Lee, *Proc. Natl. Acad. Sci. U. S. A.* **2005**, *102*, 2162.

[9] G. Muntane, I. Ferrer, M. Martinez-Vicente, *Neuroscience* **2012**, *200*, 106.

[10] A. Iwata, M. Maruyama, T. Akagi, T. Hashikawa, I. Kanazawa, S. Tsuji, N. Nukina, *Hum. Mol. Genet.* **2003**, *12*, 2625; K. S. Kim, Y. R. Choi, J. Y. Park, J. H. Lee, D. K. Kim, S. J. Lee, S. R. Paik, I. Jou, S. M. Park, *J. Biol. Chem.* **2012**, *287*, 24862; J. Levin, A. Giese, K. Boetzel, L. Israel, T. Hogen, G. Nubling, H. Kretzschmar, S. Lorenzl, *Exp. Neurol.* **2009**, *215*, 201; J. Y. Sung, S. M. Park, C. H. Lee, J. W. Um, H. J. Lee, J. Kim, Y. J. Oh, S. T. Lee, S. R. Paik, K. C. Chung, *J. Biol. Chem.* **2005**, *280*, 25216; H. Tatebe, Y. Watanabe, T. Kasai, T. Mizuno, M. Nakagawa, M. Tanaka, T. Tokuda, *Neurosci. Res.* **2010**, *67*, 341.

[11] V. Cullen, M. Lindfors, J. Ng, A. Paetau, E. Swinton, P. Kolodziej, H. Boston, P. Saftig, J. Woulfe, M. B. Feany, L. Myllykangas, M. G. Schlossmacher, J. Tyynela, *Mol. Brain* **2009**, *2*, 5; R. P. McGlinchey, J. C. Lee, *Proc. Natl. Acad. Sci. U. S. A.* **2015**, *112*, 9322; A. J. Mishizen-Eberz, R. P. Guttmann, B. I. Giasson, G. A. Day, 3rd, R. Hodara, H. Ischiropoulos, V. M. Lee, J. Q. Trojanowski, D. R. Lynch, *J. Neurochem.* **2003**, *86*, 836; A. J. Mishizen-Eberz, E. H. Norris, B. I. Giasson, R. Hodara, H. Ischiropoulos, V. M. Lee, J. Q. Trojanowski, D. R. Lynch, *Biochemistry* **2005**, *44*, 7818; D. Sevlever, P. Jiang, S. H. Yen, *Biochemistry* **2008**, *47*, 9678; W. Wang, L. T. Nguyen, C. Burlak, F. Chegini, F. Guo, T. Chataway, S. Ju, O. S. Fisher, D. W. Miller, D. Datta, F. Wu, C. X. Wu, A. Landeru, J. A. Wells, M. R. Cookson, M. B. Boxer, C. J. Thomas, W. P. Gai, D. Ringe, G. A. Petsko,

Q. Q. Hoang, *Proc. Natl. Acad. Sci. U. S. A.* **2016**, *113*, 9587; Z. Zhang, S. S. Kang, X. Liu, E. H. Ahn, Z. Zhang, L. He, P. M. Iuvone, D. M. Duong, N. T. Seyfried, M. J. Benskey, F. P. Manfredsson, L. Jin, Y. E. Sun, J. Z. Wang, K. Ye, *Nat. Struct. Mol. Biol.* **2017**, *24*, 632.

[12] A. Binolfi, A. Limatola, S. Verzini, J. Kosten, F. X. Theillet, H. M. Rose, B. Bekei, M. Stuiver, M. van Rossum, P. Selenko, *Nat. Commun.* **2016**, *7*, 10251.

[13] F. X. Theillet, A. Binolfi, B. Bekei, A. Martorana, H. M. Rose, M. Stuiver, S. Verzini, D. Lorenz, M. van Rossum, D. Goldfarb, P. Selenko, *Nature* **2016**, *530*, 45.

[14] A. M. Cuervo, L. Stefanis, R. Fredenburg, P. T. Lansbury, D. Sulzer, *Science* **2004**, *305*, 1292; M. Okochi, J. Walter, A. Koyama, S. Nakajo, M. Baba, T. Iwatsubo, L. Meijer, P. J. Kahle, C. Haass, *J. Biol. Chem.* **2000**, *275*, 390.

[15] P. Schanda, E. Kupce, B. Brutscher, *J. Biomol. NMR* **2005**, *33*, 199.

[16] F. X. Theillet, H. M. Rose, S. Liokatis, A. Binolfi, R. Thongwichian, M. Stuiver, P. Selenko, *Nat. Protoc.* **2013**, *8*, 1416.

[17] M. C. Miotto, E. E. Rodriguez, A. A. Valiente-Gabioud, V. Torres-Monserrat, A. Binolfi, L. Quintanar, M. Zweckstetter, C. Griesinger, C. O. Fernandez, *Inorg. Chem.* **2014**, *53*, 4350.

[18] O. Moscovitz, G. Ben-Nissan, I. Fainer, D. Pollack, L. Mizrachi, M. Sharon, *Nat. Commun.* **2015**, *6*, 6609.

[19] P. Kabiraj, C. A. Valenzuela, J. E. Marin, D. A. Ramirez, L. Mendez, M. S. Hwang, A. Varela-Ramirez, K. Fenelon, M. Narayan, R. Skouta, *Protein J.* **2015**, *34*, 349; F. Liu, J. L. Nguyen, J. D. Hulleman, L. Li, J. C. Rochet, *J. Neurochem.* **2008**, *105*, 2435; T. B. Sherer, R. Betarbet, C. M. Testa, B. B. Seo, J. R. Richardson, J. H. Kim, G. W. Miller, T. Yagi, A. Matsuno-Yagi, J. T. Greenamyre, *J. Neurosci.* **2003**, *23*, 10756.

[20] B. J. Mader, V. N. Pivtoraiko, H. M. Flippo, B. J. Klocke, K. A. Roth, L. R. Mangieri, J. J. Shacka, *ACS Chem. Neurosci.* **2012**, *3*, 1063.

[21] F. X. Theillet, C. Smet-Nocca, S. Liokatis, R. Thongwichian, J. Kosten, M. K. Yoon, R. W. Kriwacki, I. Landrieu, G. Lippens, P. Selenko, *J. Biomol. NMR* **2012**, *54*, 217.

[22] M. Mayzel, J. Rosenlow, L. Isaksson, V. Y. Orekhov, *J. Biomol. NMR* **2014**, *58*, 129.

[23] M. J. Smith, C. B. Marshall, F. X. Theillet, A. Binolfi, P. Selenko, M. Ikura, *Curr. Opin. Struct. Biol.* **2015**, *32*, 39.

[24] T. K. Karamanos, C. L. Pashley, A. P. Kalverda, G. S. Thompson, M. Mayzel, V. Y. Orekhov, S. E. Radford, *J. Am. Chem. Soc.* **2016**, *138*, 6271; E. Rennella, T. Cutuil, P. Schanda, I. Ayala, V. Forge, B. Brutscher, *J. Am. Chem. Soc.* **2012**, *134*, 8066.

[25] G. Fusco, M. Sanz-Hernandez, A. De Simone, *Curr. Opin. Struct. Biol.* **2018**, *48*, 49.

[26] B. Alvarez-Castelao, M. Goethals, J. Vandekerckhove, J. G. Castano, *Biochim. Biophys. Acta* **2014**, *1843*, 352.

[27] M. A. Olshina, G. Ben-Nissan, M. Sharon, *Cell Cycle* **2018**, *17*, 393; H. Solomon, B. Brauning, I. Fainer, G. Ben-Nissan, S. Rabani, N. Goldfinger, O. Moscovitz, Z. Shakked, V. Rotter, M. Sharon, *Cell Death Differ.* **2017**, *24*, 2187.

[28] C. Peng, R. J. Gathagan, D. J. Covell, C. Medellin, A. Stieber, J. L. Robinson, B. Zhang, R. M. Pitkin, M. F. Olufemi, K. C. Luk, J. Q. Trojanowski, V. M. Lee, *Nature* **2018**, *557*, 558.

[29] A. Fontana, P. P. de Laureto, B. Spolaore, E. Frare, P. Picotti, M. Zambonin, *Acta Biochim. Pol.* **2004**, *51*, 299.

[30] S. J. Hubbard, *Biochim. Biophys. Acta* **1998**, *1382*, 191.

6 Figure Legends

Figure 1: NMR characteristics of proteolytic protein processing. A) Schematic overview of endopeptidase cleavage reactions leading and new fragment N- and C-termini. **B)** NMR characteristics of 2D ^{1}H-^{15}N signal changes upon site-directed protease cleavage. **C)** Time-resolved analysis of NMR peak intensity-changes during proteolytic substrate processing. **D-F)** Time series of 2D NMR spectra of ^{15}N isotope-labeled αSyn (50 μM) reacted with 0.1 enzymatic units (U) of α-Chymotrypsin shown at indicated reaction time-points. Reference NMR spectra are in black, evolved processing states are in red. Changes of NMR signals corresponding to new N-termini are highlighted with green circles. Protease cleavage sites and new C-termini with grey and blue circles, respectively. Persisting resonances of newly generated αSyn fragments are connected by dotted lines and marked with asterisks. Residues surrounding the α-Chymotrypsin cleavage sites are indicated. **G)** Quantitative analysis of NMR signal intensity changes of selected αSyn resonances during the Chymotrypsin reaction. Kinetic profiles are fitted to exponential decay or buildup functions (shown as solid black lines). Errors due to experimental noise and timing inaccuracies at respective measurement points correspond to the dimensions of the used symbols. Note that overall rate profiles of individual cleavage reactions are internally cross-validated through measurements of different signal entities from multiple residues, of which selected sets are shown.

Figure 1 Limatola *et al.*

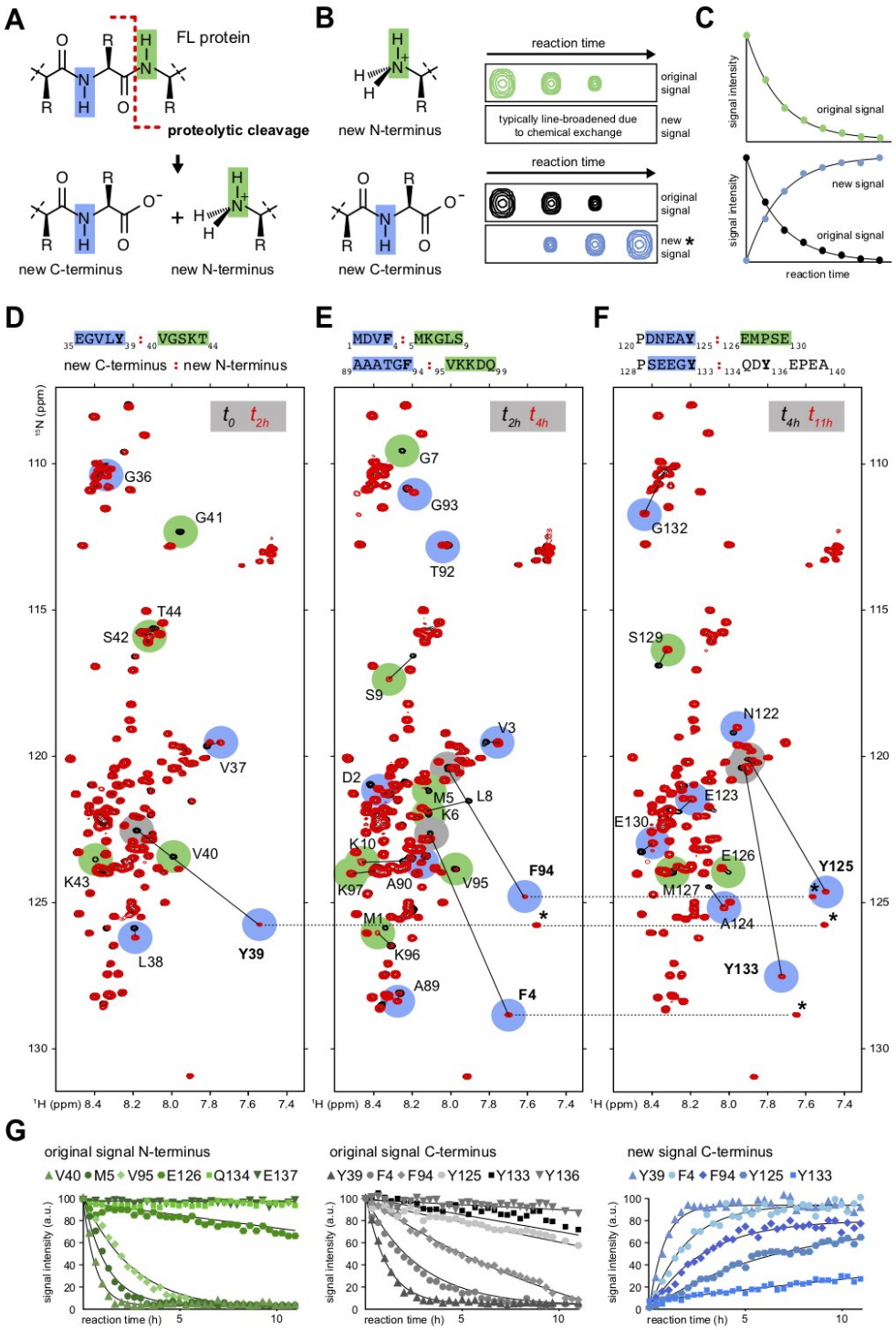

Figure 2: αSyn cleavage by Cathepsin D and 20S proteasomes. A) Coomassie-stained gels of αSyn reactions with indicated amounts of Cathepsin D at pH 6.4 (left) and pH 5.0 (right). Generated αSyn fragments are indicated. **B)** Overlay of 2D ^{1}H-^{15}N correlation spectra of reference αSyn (black) and upon Cathepsin D cleavage (red). Changes of NMR signals corresponding to new N-termini are highlighted with green circles. Protease cleavage sites and new C-termini with grey and blue circles, respectively. Residues surrounding the Cathepsin D cleavage sites are indicated. **C)** Coomassie-stained gels of αSyn in the presence of native 20S Proteasomes purified from HeLa cells. **D)** Overlay of 2D ^{1}H-^{15}N correlation spectra of reference αSyn (black) and upon 20S Proteasome cleavage (red). NMR signals of newly generated protein fragments are highlighted with blue circles.

Figure 2 Limatola *et al.*

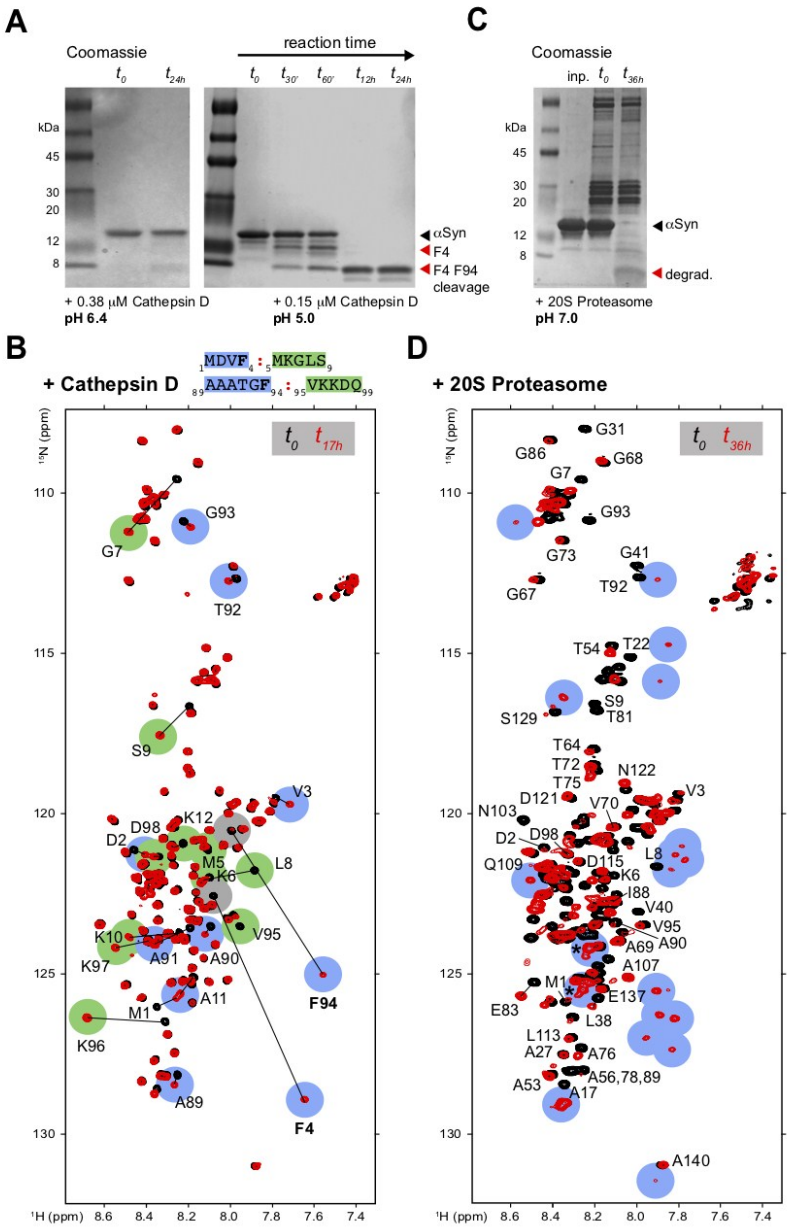

Figure 3: αSyn cleavage by endogenous proteases in SH-SY5Y cell extracts. A) Overlay of 2D ^{1}H-^{15}N correlation spectra of reference αSyn after 40 min of incubation in SH-SY5Y cell extracts obtained under non-stressed conditions at pH 5.0 (black) and after 11 h (red). We chose an early extract time-point NMR spectrum as reference not to confuse missing resonances due to exchange broadening with modulated signals due to proteolytic processing. NMR signals of newly generated protein fragments are highlighted with blue circles. Disappearing αSyn resonances and corresponding residues are indicated. **B)** Bright-field microscopy images of SH-SY5Y cells grown in absence (left) and presence of 100 nM Rotenone (right). **C)** Same experiment as in **A** but in extracts of SH-SY5Y cells treated with 100 nM of Rotenone for 72 h. Fragment resonances previously observed in unchallenged extracts are connected with dotted lines and marked with asterisks. NMR signals of newly generated cleavage products are highlighted with blue circles. **D)** Same experiment in Rotenone-challenged cell extracts prepared at pH 7.0. Tentative fragment resonances previously observed at pH 5.0 are connected with dotted lines and indicated with question marks due to slight alterations in chemical shift values, possibly caused by the differences in pH. **E)** Time-resolved Western blot analysis of αSyn cleavage by endogenous proteases in Rotenone-challenged SH-SY5Y extracts at pH 7.0. Antibodies against different αSyn epitopes reveal progressive cleavage at N- and C-terminal sites.

Figure 3 Limatola *et al.*

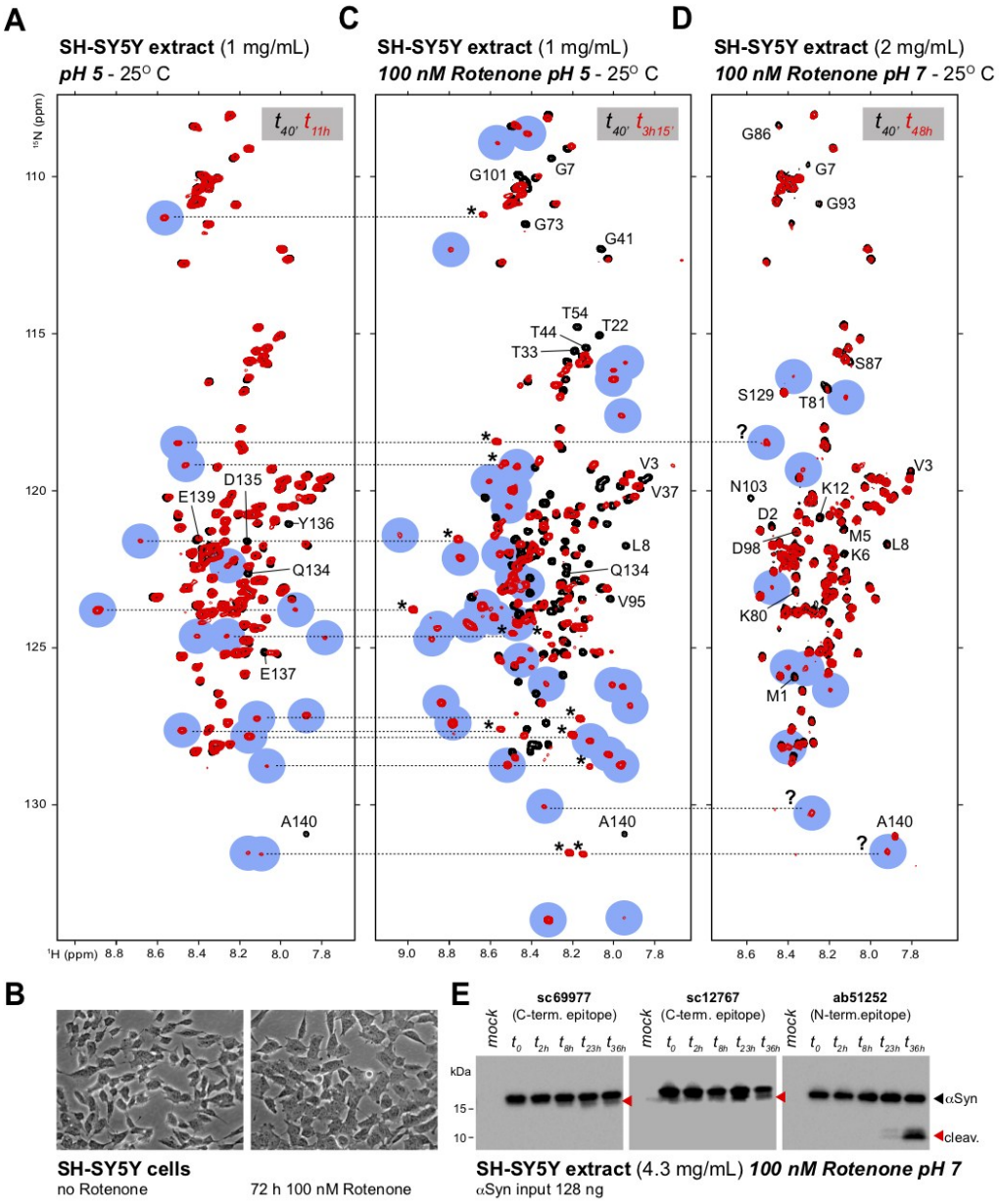

Figure 4: In-cell NMR characteristics of αSyn in SH-SY5Y cells. A) Overlay of 2D ^{1}H-^{15}N correlation spectra of reference αSyn (black) and in SH-SY5Y cells allowed to recover for 5 h after electroporation under non-challenged growth conditions, blotted at low contour levels (red). αSyn residues displaying N-terminal line-broadening are indicated. The NMR signal of a newly generated cleavage product is highlighted with a blue circle. Natural-abundance background signals of metabolites are marked with dotted circles. **B)** Same in-cell NMR experiment as in **A**, however SH-SY5Y cells allowed to recover for 12 h after electroporation (red). Chosen contour levels are the same as in **A**. Site-selective line broadening of C-terminal αSyn resonances are marked with grey circles. Truncation resonances already detected after 5 h of recovery are marked with asterisks. New fragment signals are shown in blue. Metabolite signals are indicated by dotted circles. Representative 1D traces shown on the right depict uniform line broadening of N-terminal αSyn residues (top) and site-selective, progressive reductions of C-terminal signal intensities (bottom) in the two in-cell NMR samples. Chosen contour levels for plotting in-cell NMR spectra are indicated with dashed red lines. **C)** Immunofluorescence detection of αSyn (red) in cultured SH-SY5Y cells after 5 h and 12 h recovery following protein delivery by electroporation. Clearance of transduced αSyn from manipulated cells is manifested by the progressive loss of protein signal without evident signs of aggregation such as the accumulation of bright intracellular foci. Scale bar is 10 μm. Western blots of lysates of both in-cell NMR samples (top panels) with primary anti-αSyn ab51252 antibody (N-terminal epitope). A substantial portion of delivered αSyn is found in the insoluble fraction after 5 h of recovery, including aggregated high-molecular weight species. Lysates of 12 h recovery in-cell NMR samples reveal reduced amounts of total protein, clearance of aggregated species and C-terminal truncation(s) of insoluble αSyn.

Figure 4 Limatola *et al.*